

Interference between Neutral Kaons and Their Mass Difference*†

W. A. W. MEHLHOP, S. S. MURTY, P. BOWLES, T. H. BURNETT, R. H. GOOD, C. H. HOLLAND,
O. PICCIONI, AND R. A. SWANSON

University of California, San Diego, La Jolla, California

(Received 22 April 1968)

A K^+ beam of 990-MeV/c momentum was used to produce a K^0 beam in charge-exchange collision with a copper target. By interposing an iron regenerator at a certain distance from the target and taking spark-chamber pictures of 2π decays behind the regenerator, we have observed the interference in the 2π decay mode between the K_S state produced in the original charge exchange and the K_S state (K_{LS}) produced via regeneration. The difference in phase between these K_S and K_{LS} states depends upon the proper time elapsed between production and regeneration (because of the mass difference between K_S and K_L) and can therefore be changed at will by changing the corresponding distance. The shape of the curve with the observed minimum gives us the magnitude of the mass difference, and its sign as well if the phase of the regeneration amplitude is given. In a separate work we have determined that phase from scattering experiments with charged kaons on iron nuclei. Comparing that information with the present experiment, we obtain the following results: (1) The two-pion states into which K_S and K_{LS} decay are quantum-mechanically identical. Since $|K_L\rangle$ and $|K_{LS}\rangle$ interference has already been observed, we must then expect that the time dependence of the 2π decay of K^0 will differ from that of \bar{K}^0 because of the $|K_S\rangle \rightarrow |2\pi\rangle$, $|K_L\rangle \rightarrow |2\pi\rangle$ interference. (2) The sign of the mass difference is such that K_L is heavier than K_S with a level of confidence that, barring unknown systematic errors, appears to be beyond question. (3) The value of the mass difference obtained by us is 0.42 ± 0.04 in units of \hbar/τ_S , where τ_S is the K_S mean life. (4) We have also observed the effect of the constructive interference between the scattered amplitude $f_{11}|K_S\rangle$ and the diffraction-regenerated amplitude $f_{21}|K_S\rangle$. This effect confirms that K_L is heavier than K_S .

INTRODUCTION

IT follows from the theoretical analysis of the neutral kaons that the two states K_S and K_L , which remain unchanged by the decay process, are also the states for which the mass has its simplest and narrowest distribution. The difference between the central values of the mass spectra of the two states produces oscillations (first noted by Serber¹) in the strangeness of an initially pure K^0 beam and in various phenomena associated with the regeneration.²

At the time this experiment started, there seemed to be a puzzling discrepancy between the values of the mass difference obtained by the regeneration method³⁻⁶

* Work was done in partial fulfillment of the requirements for the Ph.D. degree for Susarla S. Murty.

† The result for the sign of the mass difference has previously been given at two American Physical Society meetings [O. Piccioni, post-deadline paper, American Physical Society meeting, Washington, D. C., April 1966; R. H. Good, W. A. W. Mehlhop, O. Piccioni, R. A. Swanson, S. S. Murty, T. H. Burnett, C. H. Holland, and P. Bowles, *Bull. Am. Phys. Soc.* **11**, 767 (1966)] and has also been reported by T. D. Lee and C. S. Wu, *Ann. Rev. Nucl. Sci.* **16**, 511 (1966). Preliminary reports on this work have been made by O. Piccioni, in Proceedings of the Argonne International Conference on Weak Interactions, 1965 [Argonne National Laboratory Report No. ANL-7130 (unpublished)], p. 230; W. A. W. Mehlhop, R. H. Good, O. Piccioni, R. A. Swanson, S. S. Murty, T. H. Burnett, C. H. Holland, and P. Bowles, in *Proceedings of the Thirteenth International Conference on High-Energy Physics, Berkeley, 1966* (University of California Press, Berkeley, 1967). This work was completed under the auspices of the Atomic Energy Commission, Contract No. AEC AT (11-1), GEN 10, Project 10.

¹ R. Serber, quoted in Ref. 3. See also W. F. Fry and R. G. Sachs, *Phys. Rev.* **109**, 2212 (1958).

² A. Pais and O. Piccioni, *Phys. Rev.* **100**, 1487 (1955); M. L. Good, *ibid.* **106**, 591 (1957).

³ R. H. Good, R. P. Matson, F. Muller, O. Piccioni, W. M. Powell, H. S. White, W. B. Power, and R. W. Birge, *Phys. Rev.* **124**, 1223 (1961).

⁴ J. H. Christenson, J. W. Cronin, V. L. Fitch, and R. Turlay, *Phys. Rev. Letters* **13**, 138 (1964); *Phys. Rev.* **140**, B74 (1965).

and by the strangeness oscillation method^{7,8} (see Table I). It was then deemed opportune to have a direct quantum-mechanical confirmation that the regenerated state of K_S , which we shall call K_{LS} , decays into a two-pion state identical with the decay product of the

TABLE I. Measurements of $|\delta| = M_{K_L^0} - M_{K_S^0}$, in units of \hbar/τ_S , where τ_S is the K_S mean life.

Authors	Reference No.	$ \delta $	Year	Method
Fitch <i>et al.</i>	7	1.9 ± 0.3	1961	Strangeness oscillation
Camerini <i>et al.</i>	8	1.5 ± 0.2	1962	method
Erratum to Ref. 8	9	0.88 ± 0.2	...	
Meisner <i>et al.</i>	10	0.65 ± 0.30	1965	
Camerini <i>et al.</i>	11	0.50 ± 0.16	1966	
Hill <i>et al.</i>	12	0.62 ± 0.16	1966	
Good <i>et al.</i>	3	$0.84_{-0.22}^{+0.29}$	1961	Coherent regeneration
Christenson <i>et al.</i>	4	0.55 ± 0.10	1965	method
Fujii <i>et al.</i>	5	0.82 ± 0.12	1964	
Vishnevsky <i>et al.</i>	6	0.82 ± 0.14	1965	
Alff-Steinberger <i>et al.</i>	13	0.445 ± 0.034	1966	Interference methods
V. L. Fitch <i>et al.</i>	14	0.50 ± 0.10	1965	involving CP-violating decay $KL \rightarrow 2\pi$
Bott-Bodenhausen <i>et al.</i>	15	0.48 ± 0.024	1966	
Aubert <i>et al.</i>	16	0.47 ± 0.20	1964	Time dependence of leptonic decay
Baldo-Ceolin <i>et al.</i>	17	$0.15_{-0.50}^{+0.35}$	1965	
Franzini <i>et al.</i>	18	0.5	1965	
This experiment		0.42 ± 0.04	1968	Interference between K_S, K_{LS}

⁵ T. Fujii, J. V. Jovanovich, F. Turkot, and G. T. Zorn, *Phys. Rev. Letters* **13**, 253 (1964).

⁶ M. E. Vishnevsky, N. D. Galanina, Yu A. Semenov, P. A. Krupchitsky, V. M. Berezin, and V. A. Murisov, *Phys. Letters* **18**, 339 (1965).

⁷ V. L. Fitch, P. A. Piroué, and R. B. Perkins, *Nuovo Cimento* **22**, 1160 (1961).

⁸ U. Camerini, W. F. Fry, J. Gaidos, H. Huzita, S. Natali, R. Willmann, R. Birge, R. Ely, W. Powell, and H. White, *Phys. Rev.* **128**, 362 (1962).

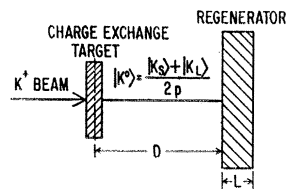


FIG. 1. Schematic drawing showing the principle of the experiment.

original K_S . A clear proof of this identity would derive from the interference of these K_S and K_{LS} states.

At the time of writing, the mentioned discrepancy has disappeared,⁹⁻¹⁸ so that our experimental evidence for the K_S , K_{LS} identity confirms that no such disagreement should exist, and strengthens our confidence in the mixture theory of neutral kaons.

To explain the principle of our experiment, we refer to the schematic drawing of Fig. 1. A pure K^0 beam leaves the charge-exchange target and, after crossing a distance D , collides with the regenerator plate of thickness L .

At the exit of the plate L , the K_S component of the beam has an amplitude

$$\psi_S = \exp[(ik_S - 1/2\Lambda)(D+L) - L/2\mu] \quad (1)$$

and at the exit of the plate L an undeflected, transmission-regenerated component is produced with an amplitude³

$$\begin{aligned} \psi_{LS} &= A(L) \exp[ik_S L + ik_L D - L/2\mu] \\ &= A(L) \exp[ik_S(D+L) - i\delta D/\Lambda - L/2\mu], \end{aligned} \quad (2)$$

where k_L and k_S are momenta of the K_L and K_S mesons, respectively.

$\delta = (M_L - M_S)c^2\tau_s/\hbar$ is the K_L and K_S mass difference in units of \hbar/τ_s , where τ_s is the mean life.

μ = nuclear absorption mean free path which is equal for K_L and K_S = 14.1 cm.^{5,19}

⁹ U. Camerini *et al.*, erratum to Ref. 8; Phys. Rev. (to be published).

¹⁰ G. W. Meisner, B. B. Crawford, and F. S. Crawford, Jr., Phys. Rev. Letters **16**, 278 (1965).

¹¹ U. Camerini, D. Cline, J. B. English, W. Fischbein, W. F. Fry, J. A. Gaidos, R. C. Hantman, R. H. March, and R. Stark, Phys. Rev. **150**, 1148 (1966).

¹² D. G. Hill, D. K. Robinson, M. Sakitt, J. Canter, Y. Cho, A. Engler, H. E. Fisk, R. W. Kraemer, and C. M. Melzer, in *Proceedings of the Thirteenth International Conference on High-Energy Physics, Berkeley, 1966* (University of California Press, Berkeley, 1967); magnitude of the K_L - K_S mass difference.

¹³ C. Alf-Stenberger, W. Heuer, K. Kleinknecht, C. Rubbia, A. Scribano, J. Steinberger, M. J. Tannenbaum, and K. Tittel, Phys. Letters **20**, 207 (1966); **21**, 595 (1966).

¹⁴ V. L. Fitch, R. F. Roth, J. S. Russ, and W. Vernon, Phys. Rev. Letters **15**, 73 (1965).

¹⁵ M. Bott-Bodenhausen, X. De Bouardix, D. G. Cassel, D. Dekkers, R. Felst, R. Mermod, I. Savin, P. Scharif, M. Vivargent, T. R. Willits, and K. Winter, Phys. Letters **20**, 212 (1966); **23**, 277 (1966).

¹⁶ B. Aubert, L. Behr, J. P. Lowys, P. Mittner, and G. Pascand, Phys. Letters **10**, 215 (1964).

¹⁷ M. Baldo-Ceolin, E. Calimani, S. Ciampollio, C. Fillippi-Filosofo, H. Huzita, F. Mattioli, and G. Miari, Nuovo Cimento **38**, 684 (1965).

¹⁸ P. Franzini, L. Kirsch, P. Schmidt, J. Steinberger, and R. J. Plano, Phys. Rev. **140**, B217 (1965).

¹⁹ Actually, because of the real part of the elastic scattering

Λ = decay mean free path for K_S = 3.98 cm for p = 760 MeV/ c .

$A(L) \exp(ik_S L)$ represents the K_S amplitude regenerated by a unity K_L amplitude of zero phase arriving at the entrance of the regenerator of thickness L .

$$A(L) = if_{21} N \lambda \Lambda \left[\frac{\exp(-i\delta L/\Lambda) - \exp(-L/2\Lambda)}{-i\delta + \frac{1}{2}} \right]. \quad (3)$$

N = number of nuclei per cubic centimeter in iron = 0.85×10^{23} nuclei/cm³.

$\lambda = K^0$ wavelength = 1.63 F for p = 760 MeV/ c .

f_{21} = regeneration amplitude in the forward direction = $\frac{1}{2}(f^+ - f^-)$, where f^+ and f^- are the amplitudes for forward scattering of K^0 and \bar{K}^0 .

Note that these formulas are the same as they were when K_S , K_L were identified with K_1 , K_2 , respectively [K_1 , $K_2 = (K^0 \pm \bar{K}^0)/\sqrt{2}$], because

$$\begin{aligned} f^+ p |K^0\rangle - f^- q |\bar{K}^0\rangle \\ = \frac{1}{2}(f^+ + f^-)(p |K^0\rangle - q |\bar{K}^0\rangle) \\ + \frac{1}{2}(f^+ - f^-)(p |K^0\rangle + q |\bar{K}^0\rangle). \end{aligned}$$

The total amplitude at the exit of plate L is therefore given by

$$\begin{aligned} \psi(D+L) &= \psi_S + \psi_{LS} \\ &= \left[\exp\left(-\frac{D+L}{2\Lambda}\right) + A(L) \exp\left(-\frac{i\delta D}{\Lambda}\right) \right] \\ &\quad \times \exp\left[-\frac{L}{2\mu} + ik_S(D+L)\right]. \end{aligned}$$

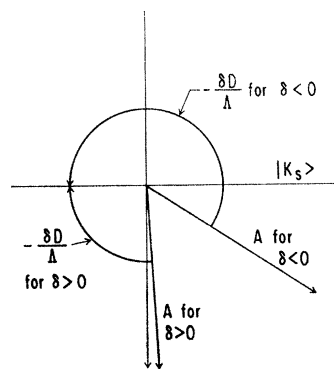


FIG. 2. Phase relation between the amplitudes of $|K_S\rangle$ and of $|K_{LS}\rangle$. Angles shown are proportional to distances D of Fig. 1.

amplitude, $f_{11}(0) = f_{22}(0) = \frac{1}{2}(f^+ + f^-)$, the wavelength of the particle in iron differs from its value in vacuum, so that μ should be a complex number. If n is the index of refraction of the medium,² the propagation of the wave through a dense medium is, of course, given by e^{inkx} , where $n - 1 = 2\pi N f_{11}(0)/k^2$. Clearly, $n - 1$ has a real part [as well as an imaginary part $-1/(2\mu k)$] which produces a change of phase of the particle as it goes through the medium, with respect to the vacuum. Since the momentum k differs from K_L to K_S , such a phase change also differs from K_L to K_S . However, we have neglected this point because the resulting difference between K_L and K_S is very small.

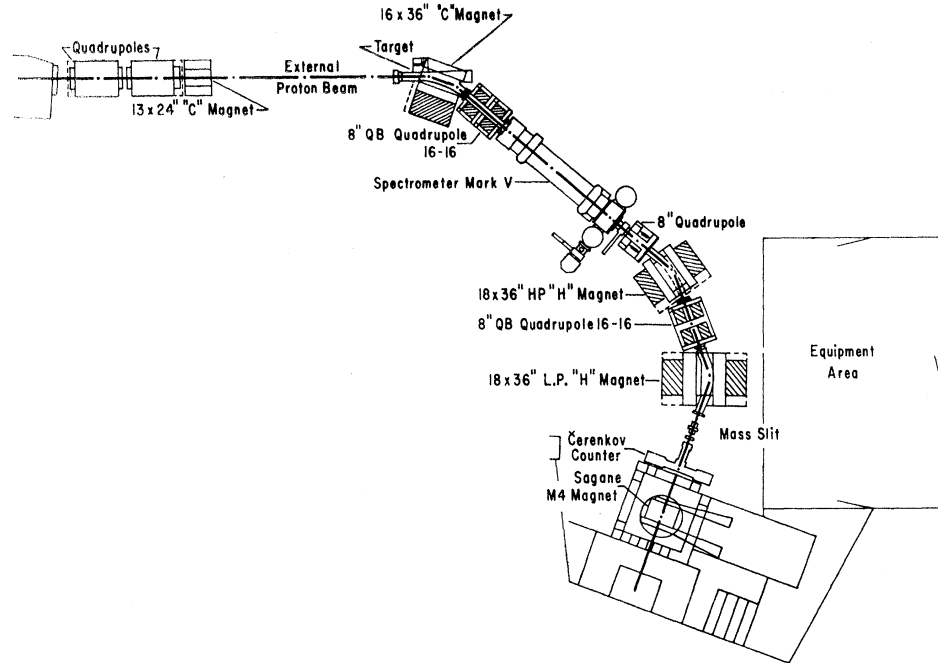


FIG. 3. Plan view of the layout of the beam components on the Bevatron floor.

The resultant K_S intensity is given by $I = |\psi_S + \psi_{LS}|^2$.

$$I = \exp(-L/\mu) \left[\exp\left(-\frac{D+L}{\Lambda}\right) + |A|^2 + 2 \exp\left(-\frac{D+L}{2\Lambda}\right) |A| \cos\left(\arg A - \frac{\delta D}{\Lambda}\right) \right]. \quad (4)$$

TABLE II. Optical properties of the K^+ beam.

Momentum (MeV/c)	990 MeV/c
Solid angle (msr)	2.3
Length from external proton beam target to copper charge-exchange target	602 in.
Horizontal acceptance angle (mrad)	128
Vertical acceptance angle (mrad)	17.9
Total momentum width	5%
Horizontal magnification (first focus)	≈ 4.73
Horizontal magnification (second focus)	≈ 6.13
Vertical magnification	≈ 1.08
Target location	External beam third focus
Target material	Platinum
Target size	$\frac{1}{8}$ in. vertically $\frac{1}{4}$ in. horizontally $2\frac{1}{2}$ in. length
Production angle	2°
Separation at 990 MeV/c: $K-\pi$ separation/vertical image size	≈ 2.4
Pion rejection	$\approx 10^2$
Flux (990 MeV/c)	$12\,000 K^+$ per 5×10^{11} protons
$K_S(\pi^+, \pi^-)$ decays detected ($p = 760$ MeV/c)	$2.6 \exp(t/\tau_S)$ per $10^4 K^+$

The mean life of the long-lived K_L has been assumed to be infinite, and the regeneration in the charge-exchange target itself has been neglected. The effect of the CP -violating decay of K_L into two pions was also found completely negligible.

If the states K_S and K_{LS} are quantum-mechanically identical, the number of 2π decays beyond the regenerator L will be proportional to I . If not, it will be proportional to $|\psi_S|^2 + |\psi_{LS}|^2$. The difference in phase between ψ_{LS} and ψ_S is

$$[\arg \psi_{LS} - \arg \psi_S] = [\arg A - \delta D/\Lambda],$$

which is 180° for an appropriate value of the distance D .

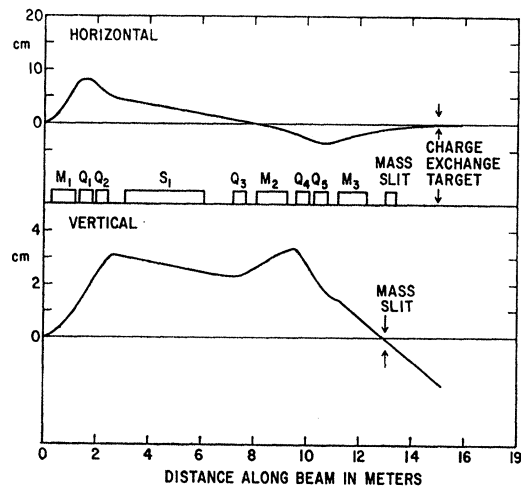


FIG. 4. Horizontal and vertical ray diagrams of the beam from a point target for the central momentum.

TABLE III. Description of components.

Component	Description	Distance* from last component (in.)	Distance* from target (in.)	Operating value	Comments
<i>T</i>	External proton beam target	0	0	2° production angle	$\frac{1}{4}$ in. (<i>H</i>) $\times\frac{1}{8}$ in. (<i>V</i>) \times 2.5 in. long; rotated 1°
<i>M1</i>	Bending magnet	28	28	19.4 kG, 38° bend	16 \times 36 in. C magnet
<i>Q1</i> <i>Q2</i>	Quadrupole doublet	{44 26}	{72 96}	1077 G/cm 744 G/cm	Horizontal focus Vertical focus } 8 \times 16 \times 16 in.
<i>VS</i>	Velocity separator	95	191	580 kV/2.5 in.	10 ft separator
<i>Q3</i>	Quadrupole lens	112	303	270 G/cm	Horizontal focus 8 \times 16 in.
<i>M2</i>	Bending magnet	48	351	14.93 kG, 30° bend	18 \times 36 in. HP <i>H</i> magnet
<i>Q4</i> <i>Q5</i>	Quadrupole doublet	{48 24}	{399 423}	557 G/cm 723 G/cm	Vertical focus Horizontal focus } 8 \times 16 \times 16 in.
<i>M3</i>	Bending magnet	69	472	19.81 kG, 40° bend	18 \times 36 in. LP <i>H</i> magnet
<i>S</i>	Mass slit	51	523		
<i>T¹</i>	Copper charge-exchange target	79	602		Charge-exchange target

* Referred to the center of the respective component.

$\arg A$ is the sum of four nonzero phases [see Eq. (3)]. The angle of the bracketed quantity B is -72° (numerator) $-(-45^\circ)$ (denominator), that is, -27° , for $\delta > 0$, and just changes sign if δ does. Thus, if the product of if_{21} were real, the value of $\arg A$ would only change sign with δ . Obviously, the angle $\delta D/\Lambda$ also changes sign with δ , so that $\cos(\arg A - \delta D/\Lambda)$ would be independent

of the sign of δ . Fortunately, $\arg if_{21} \simeq -60^\circ$, so that the situation is as shown in Fig. 2.

The ratio of the amplitudes ψ_{LS} and ψ_S is $|A|/\exp[-(D+L)/2\Lambda]$, which points to an important feature of this experiment; namely, as the distance D increases, the thickness L of the regenerator can be reduced so that the amplitude of K_S from the target and

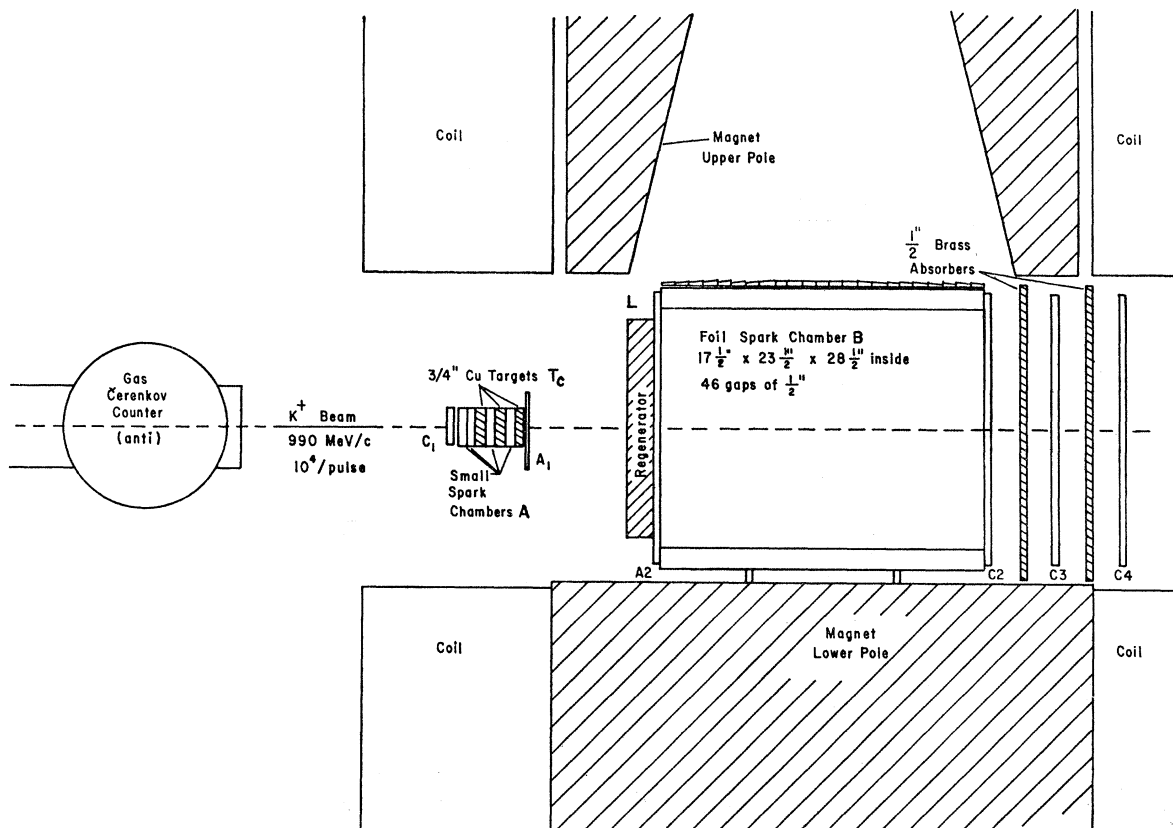


FIG. 5. Side view of the experimental setup. The slit counter and the water Čerenkov counter are not shown in the figure.

TABLE IV. Target-regenerator spacing for different geometries.^a

Rolls	3-cm run				Rolls	6-cm run			
	D_1 (cm)	D_2 (cm)	D_3 (cm)	L (cm)		D_1 (cm)	D_2 (cm)	D_3 (cm)	L (cm)
190-192	12.60	9.80	7.00	0.0	198-207	12.20	8.75	5.30	0.0 (close geometry)
107-114	23.70	20.9	18.10	7.6	211-213	24.25	20.8	17.35	7.6
92-106	23.70	20.9	18.10	5.1	269-275	28.90	25.50	22.05	7.6
53-92	31.30	28.50	25.70	5.1	275-278	19.45	16.0	12.55	7.6
115-136	38.60	35.8	33.0	2.9	213-219	32.85	29.4	25.95	5.1
157-161	38.60	35.8	33.0	2.9	279-291	35.35	31.9	28.45	3.8
162-188	42.70	39.90	37.1	1.6	219-268	37.45	34.0	30.55	2.9
					327-356	43.75	40.30	36.85	1.6
					357-367	42.95	39.50	36.05	7.6 (far geometry)

^a D_i ($i=1, 2, 3$) is the distance from target i to the downstream side of the regenerator. Target 1 is the upstream target. L is the regenerator thickness.

of K_{LS} from the regenerator remain comparable in value, thus maximizing the effect of the destructive interference.

EXPERIMENTAL PROCEDURE

The external proton beam of the Bevatron, having an energy of 5.0 BeV, impinges on a platinum target (see Table II). The sequence of magnets and the electrostatic separator used to transport the charged K beam²⁰ of momentum 990 MeV/ c from the platinum target to the copper charge-exchange target is shown in Fig. 3. The horizontal and vertical ray trajectories from a point target, for the central momentum, are shown in Fig. 4. The optical properties of the beam are tabulated in Table II, and the beam components are given in Table III.

The beam was made approximately parallel in the vertical plane by the first two quadrupoles $Q-1$ and $Q-2$. It then passed through the electrostatic separator which was 10 ft long with a gap of $2\frac{1}{2}$ in. and a total difference of electrical potential of 580 kV which deflected kaons by an angle of 2.7 mrad with respect to the pions. At the slit, the separation of kaons from pions was 0.79 cm and the full width at half-maximum of the image was 0.4 cm. The horizontal and vertical acceptances were limited by the quadrupole $Q-1$ and the separator electrodes, respectively.

At the entrance of the bending magnet $M-2$, there was an intermediate horizontal focus. At the same place, the pole tips of $M-2$ were corrected with shims in order to provide a gradient of H_y (y axis is vertical) proportional to the horizontal displacement x from the optic axis ("sextupole correction"). Because of the first bending magnet M_1 at the intermediate focus, there was a linear relation between x and the momentum of particles passing at distance x from the axis; thus particles of different momentum passed through different gradients. In other words, a chromatic correction was obtained, resulting in a better vertical image at the mass slit.

²⁰ We appreciate very much the help of Dr. George H. Trilling and Dr. J. A. Kadyk of Lawrence Radiation Laboratory in the design work of the K beam used in this experiment.

After the magnet $M-2$, the two quadrupoles $Q-4$ and $Q-5$ focused the beam vertically on the uranium slit which distinguished the image of kaons from the images of pions and protons.

After this, the beam continued and reached the charge-exchange target. The layout of the counters and spark chambers from this point on is shown in Fig. 5.

The first spark chamber A (see Fig. 5) gave the picture of the trajectory of the incoming kaon and, in particular, allowed us to determine with accuracy the position of the charge-exchange collision. The second chamber B gave the picture of the two-pion decay, allowing for the measurement of direction and curvatures of each of the two prongs in a magnetic field of an average value of 10 000 G.

The charge-exchange collision target, made of copper, was inserted among the elements of the first spark chamber A. For a first set of pictures, the charge-exchange collision target was made of three 1-cm-thick plates (hereafter referred to as 3-cm run). For a second set of pictures, it was made of three 2-cm plates (6-cm run). The whole complex of charge-exchange target and the first spark chamber could be moved in the direction parallel to the incoming K^+ beam to allow the taking of pictures at various distances between the charge-exchange target T_e and the regenerator L .

The presence of three charge-exchange targets, rather than one, made the experiment more efficient in that it gave, at the same time, data at three values of target-regenerator distance, though with somewhat reduced efficiency for each one because of nuclear interactions. The distances and the regenerator thicknesses used are given in Table IV. As mentioned before, for each setting, the amplitude of the residual K_S wave was matched, for the central momentum, to the amplitude of the regenerated wave. However, data were also taken with no regenerator at a small regenerator-charge-exchange target spacing (hereafter referred to as close-geometry run) and with a large regenerator at a large regenerator-target spacing (hereafter referred to as far-geometry data), where the original K_S amplitude was negligible, in order to have two important calibrating points.

TABLE V. Details of counters.

Counter	Type	Dimensions	Function
Slit counter	Scintillator		Requires that the charged particles go through the mass slit.
<i>W</i>	H ₂ O Čerenkov		Requires particles with velocity $\beta > 0.75$ (rejects protons).
<i>G</i>	Čerenkov Freon gas	5 in. diameter, 26 in. length	Rejects particles lighter than <i>K</i> meson.
<i>C</i> ₁	Scintillator	4×5× $\frac{1}{2}$ in.	Ensures that the charged particles entered the targets.
<i>A</i> ₁	Scintillator	4×5× $\frac{1}{2}$ in.	In anticoincidence, requires that no charged particle came out of the targets.
<i>A</i> ₂	Scintillator	34.5×20.5× $\frac{1}{2}$ in.	In anticoincidence, requires that no charged particle came out of regenerator.
<i>C</i> ₂	Scintillator	40.0×20.5× $\frac{1}{2}$ in.	All these three counters connected in coincidence, require that one of the charged decay products penetrate 1 in. of brass plus $1\frac{1}{2}$ in. of plastic scintillator.
<i>C</i> ₃	Scintillator	40.0×20.5× $\frac{1}{2}$ in.	
<i>C</i> ₄	Scintillator	40.0×20.5× $\frac{1}{2}$ in.	

Spark Chambers

A small spark chamber with four 2-gap sections (spark chamber A) was used to locate the point of charge exchange of *K*⁺ mesons. Each of the sections was 3×5 in. inside and had two $\frac{1}{4}$ -in. gaps.

A large foil spark chamber (spark chamber B) was used to detect the *K*_S⁰ meson decay pions and measure their momenta. It consisted of 46 $\frac{1}{2}$ -in. gaps, each 17.5×28.5 in. inside. The over-all length of the chamber was 23.75 in. The wall frames were made of 1.5-in. Lucite.

The experiment used different cameras for the top and side view. The correlation was made by photographing Nixie tubes in both views. Each of the cameras was built in our laboratory on the following principle. A fast-response motor drove a capstan drum which moved the unperforated 35-mm film. The same motor provided both the accelerating and the braking torque. A dc generator (tachometer) fastened to the shaft of the motor itself furnished a signal which indicated how much the film had advanced and caused a transistor circuit to reverse the motor torque at the right time. The mechanical parts of the cameras were thus rather simple. A rate of 13 frames/sec was easily achieved. The amount of advancement of the film could be varied by

changing the value of a few resistors and the dimensions of the film window.

Details of the counters are given in Fig. 5 and Table V. The spark chambers were triggered by $\bar{A}_1 C_1 C_2 C_3 C_4 \bar{A}_2$. The beam spill during the experiment was 800 msec. The repetition rate was one every 6–10 sec. On the average, about three pictures were taken per Bevatron pulse.

DATA REDUCTION

All 200 000 pictures taken during the experiment were scanned for *V* events in the spark chamber B. 29 764 *V* events were observed on the scan table and measured. Of the measured pictures, 4450 were rejected and were then remeasured. 1356 *K*_S events and 4587 *K*_L events were recognized.

The computer program KADAP finds the particle trajectory that comes closest to the set of observed points on the track. The assumed error of measurement is a function of the track angle. Many functions were compared against data samples. The best function was

$$\sigma = 0.036 (1 + \sin^4 \theta) \text{ cm,}$$

$$\theta = \text{angle of track to plate normal.}$$

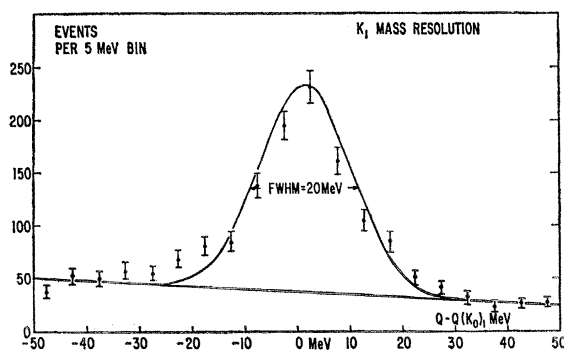


FIG. 6. ΔQ ($=Q - Q_{K_S^0}$) distribution of observed *K*_S⁰ in the first 10 cm (about 2.5 mean lives at our peak *K*⁰ momentum of 760 MeV/*c*) of the foil chamber for both 6-cm and 3-cm runs combined together.

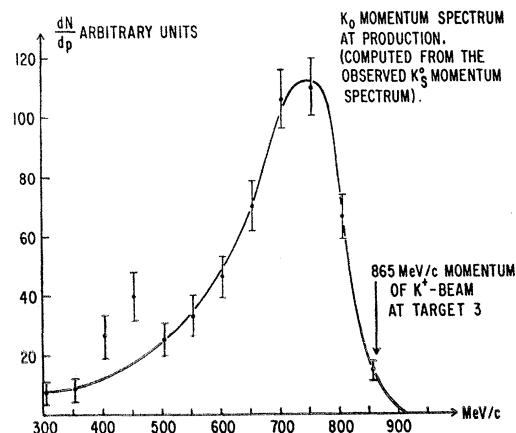


FIG. 7. *K*⁰ momentum spectrum at production computed from the observed *K*_S⁰ momentum spectrum.

TABLE VI. Number of events having $1.0 < \cos(\theta p/760) < 0.998$ (uncorrected number of transmission events).^a

T limits \ Y/L	7.60/0	16.0/7.6	20.8/7.6	24.5/7.6	20.8/5.1	28.0/5.1	31.0/3.8	34.0/2.9	38.5/1.6	38.5/7.6
1-2	59									
2-3	52									
3-4	16	19								
4-5		18	3		12					
5-6		5	3	3	12					
6-7		2	8	14	3	14	1			
7-8			6	10	1	38	10	13		
8-9			3	10		19	24	46	2	2
9-10				4		10	22	42	17	17
10-11						7	6	26	28	29
11-12						2	1	11	25	19
12-13							4	5	9	12
13-14									10	5
14-15									3	2
15-16									1	1
Total	127	44	23	41	28	90	68	143	95	87 = 746

^a T is the proper-time value. Y is the distance from center of center target to downstream side of regenerator L in cm.

TRACK FIT, a subroutine of KADAP, minimizes χ^2 with respect to track-origin parameters K , θ , α , X , and Y , where $K = 1/p_{BeV/c}$, θ , α are the spatial angles, and X , Y are the spatial coordinates. Since the actual fitting was done in the plane of projection, it was not necessary for the operator to measure the corresponding points in both views.

The program also computes the regeneration angle, which is the angle between the momentum vector of K_S and the line of flight of K^0 . The approximation was made of taking for this line the line from the charge-exchange point to the point where the P_{K_S} vector intersected the middle plane of the regenerator.

The time of flight $T = (D+L)/\Lambda$ for each K_S^0 was also computed.

RESULTS AND DISCUSSIONS

The width of the Q value and momentum distributions (Figs. 6 and 7) suggested selection criteria based

on these parameters; namely, an event should lie within the first 10 cm (≈ 2.5 mean lives) of the B chamber, and have a Q which differs from the Q value of the K^0 by no more than ± 30 MeV, and a momentum that should lie between 600 and 900 MeV/ c . We emphasize that such criteria can be chosen at will, because the (variable) position of the K^0 source does not affect the measurement errors of events that originate behind the regenerator in the B chamber.

The useful solid angle for the neutral kaons does, of course, change with the position of the K^0 source. Because of this, we have always taken as significant the ratio of K_S decays to K_L decays. For each setting (a setting is characterized by a distance D and a regenerator thickness L ; see Table IV) we assume that N_i^0 , the number of K^0 emitted from the charge-exchange target into our usable solid angle, is proportional to N_i^L , namely, the observed number of K_L decays in the B chamber. We write then $N_i^0 = CN_i^L$, where C depends

TABLE VII. Number of events having $0.998 < \cos(\theta p/760) < 0.98$ (diffraction).^a

T limits \ Y/L	7.60/0	16.0/7.6	20.8/7.6	24.5/7.6	20.8/5.1	28.0/5.1	31.0/3.8	34.0/2.9	38.5/1.6	38.5/7.6
1-2	18									
2-3	9									
3-4	1	13								
4-5	2	17	2		10					
5-6		13	10	4	19	1				
6-7		3	11	16	4	21				
7-8			1	13	3	32	13	10		
8-9			3	3		24	16	29	4	
9-10				2		10	15	27	18	3
10-11			1	1		5	9	20	32	12
11-12				1		1	2	12	25	16
12-13							2	2	20	17
13-14									5	8
14-15									8	7
15-16									1	2
Total	30	46	28	40	36	94	57	100	113	66 = 610

^a T is the proper-time value. Y is the distance from center of center target to downstream side of regenerator L in cm.

TABLE VIII. Corrected number of transmission events.

T bin limits	Events having $\cos(\theta p/760) > 0.998$	Events having $0.998 < \cos(\theta p/760) < 0.98$	$\Delta N_{TR} = (1.0 \text{ to } 0.998) - 0.416 \times (0.998 \text{ to } 0.98)$	Comments
1-2	59	18	51.50	Close-geometry data
2-3	52	19	44.09	
3-4	16	1	15.58	
3-4	19	13	13.59	Interference part of data
4-5	33	29	20.94	
5-6	23	47	3.45	
6-7	42	55	19.12	
7-8	78	72	48.05	
8-9	104	79	71.14	
9-10	95	72	65.05	
10-11	67	68	38.72	
11-12	39	41	21.94	Far-geometry data
8-9	2	3	0.752	
9-10	17	12	12.00	
10-11	29	16	22.30	
11-12	19	17	11.93	
12-13	12	8	8.67	
13-14	5	7	2.09	
14-15	2	2	1.17	

upon the thickness of the regenerator. Both N_i^0 and N_i^L are functions of the momentum p .

An important point was to determine once and for all the spectrum of K^0 's produced by charge exchange. This was accomplished by measuring K_S events at a close geometry with no regenerator. With the proper correction for K_S decay, this setting furnished the production spectrum $S(p) = dN^0/dp$ (see Fig. 7). We assumed that this spectrum was essentially determined by the geometry of the charge-exchange target and by the anticoincidence counter following the target, and that the distance D did not appreciably affect it. We have confirmation of this in the far-geometry data.

Similarly, we assumed that the relative probabilities, R_1 , R_2 , and R_3 , for a K^0 to originate in the first, second, or third copper target, respectively, did not change with D . For better accuracy, we then determined these probabilities from the K_L decay data from all settings grouped together, observing the origin in the spark chamber A. Then, for each setting i , from the number of K_L decays N_i^L , we computed the expected number of K^0 's produced, for example, in the first Cu target, in the useful solid angle within the momentum range p and $p+dp$, namely, $CR_1N_i^L S(p)dp$. From this quantity we computed, grouping all settings together, the number of K^0 's produced in the interval T , $T+\Delta T$, where T is the proper time from the production point to the exit of the regenerator.²¹ We indicate this number as $\Delta N^0(T)$. This was our normalization.

For each K_S decay found, the measured momentum and the observed charge-exchange point allowed us to determine the proper time T (from the exchange point to the downstream side of the regenerator). The number of K_S events found in the interval T , $T+\Delta T$, will be indicated by $\Delta N_S(T)$.

The intensity of the K_S state in the interval T , $T+\Delta T$, after the regenerator, is thus given by $\Delta N_S(T)/\Delta N^0(T)$, and it should reproduce the function of Eq. (4). However, to make full use of our experimental information and to reduce the statistical error, we have grouped together data taken with somewhat different regenerator thicknesses (see Tables VI-VIII) for the same values of T . Thus, our intensity curve departs somewhat from the mathematical form of Eq. (4); namely, it is the superposition of few terms of the type (4), each with a different value of L . The expected curve is computed

²¹ T is not the actual life-span of the K^0 in a given event; its value is uniquely computed from the momentum and the target-regenerator spacing

$$T = (D+L/pc)(Mc^2/c\tau).$$

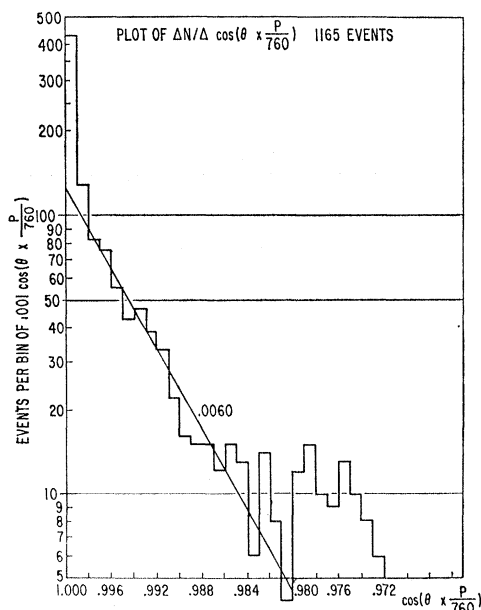
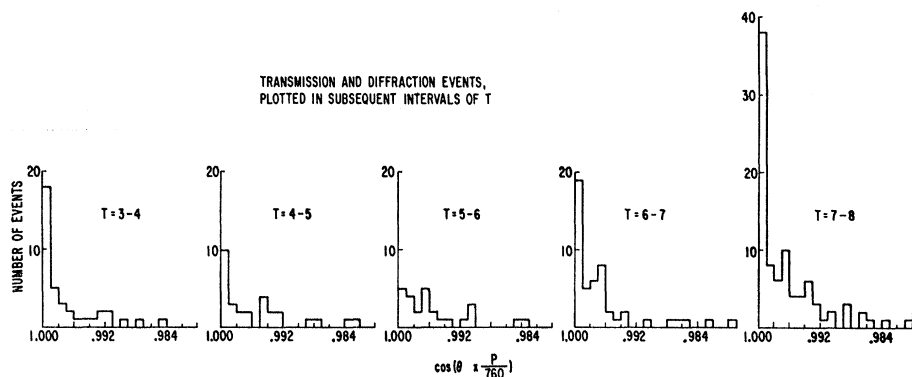


Fig. 8. Angular distribution of all the events.

FIG. 9. Transmission and diffraction events plotted in subsequent intervals of $T = (D+L)/\lambda$. Notice the absence of the forward transmission peak for the events between $T=5$ and $T=6$ which shows rather clearly the effect of the interference independently from the K_L normalization.



accordingly, so that the comparison has its full significance.

Only the data taken at "close geometry" and "far geometry" have been left as separate groups because they were taken with a regenerator thickness too different from the optimum value to study the interference effect. These data are plotted separately in Figs. 10 and 12.

Experimentally, to select the events to which Eq. (4) applies, we had to distinguish two categories: (1) events

due to the original plus the transmission-regenerated amplitude at zero angle; (2) events due to the nuclear scattered plus nuclear regenerated amplitude, at finite angles.

Figure 8 shows the angular distribution for all events plotted as a function of $\cos[\theta \times p(\text{BeV}/c)/0.76]$ so as to make it momentum-independent. The distribution shows that a "background" due to scattering events is present in the interval 1.0 to 0.998 (Table VI) in an amount equal to 0.416 of the number of events in the interval 0.998 to 0.980 (Table VII). Thus, we took for the number of nonscattered transmission events $\Delta N_{\text{TR}} = (1.0 \text{ to } 0.998) - 0.416 \times (0.998 \text{ to } 0.98)$ (Table VIII), where the parentheses represent the number of events in the specified interval. The scattering-regenerated events which were selected with the criterion that the angle should be larger than some minimum value could

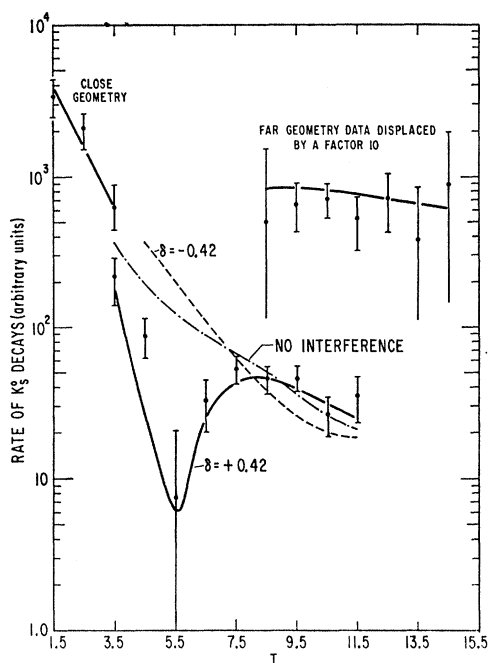


FIG. 10. (6-cm data and 3-cm data combined). Rate of K_S^0 decays versus distance T (expressed as time of flight in units of τ_s^0). Here we used the regeneration phase $\varphi_{21} = -155.5^\circ$ and amplitude $|f_{21}| = 12.7 F$ ($p = 785 \text{ MeV}/c$) obtained from the scattering experiment (see Table IX). The "close geometry" data and "far geometry" data have been taken with a regenerator thickness too different from the optimum value to study the interference effect. Thus, they have not been lumped together with the other data for equal values of T . The computed curves for all geometries are, of course, determined by the same parameters and the fitting procedure fits all points.

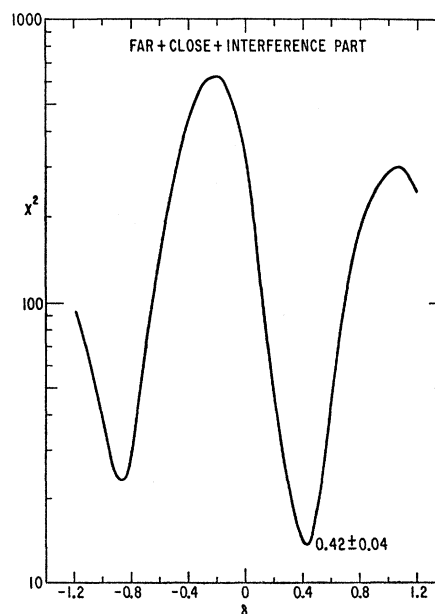


FIG. 11. Plot of χ^2 versus 6-cm and 3-cm data combined. $|f_{21}| = 12.7 F$ ($p = 785 \text{ MeV}/c$), $\varphi_{21} = -155.5^\circ$ from scattering experiment. The error quoted on δ does not include the errors on $|f_{21}|$ and φ_{21} .

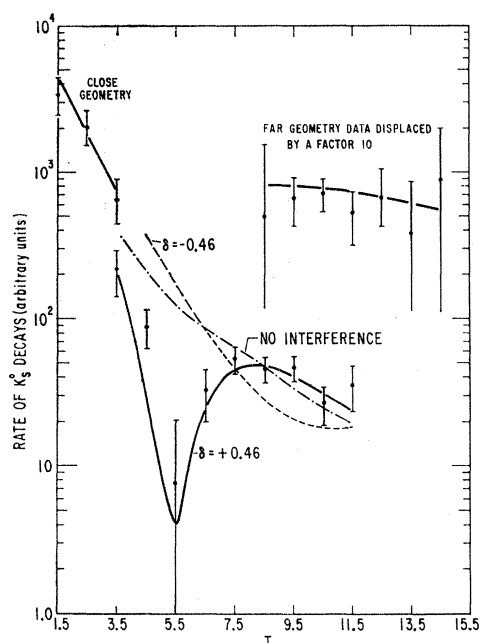


FIG. 12. Rate of K_S^0 decays versus distance. Here we assume $\delta = 0.46$ (from Refs. 13 and 15) and then make a fit for $|f_{21}|$ and φ_{21} . We obtain $|f_{21}| = 11.25 \pm 0.9$ F and $\varphi_{21} = 150.0^\circ \pm 11.5^\circ$, which agrees with the values obtained from scattering experiment (see Table IX).

of course also furnish our normalization, but the accuracy which we would obtain in this way is not as good as that obtained from the K_L decay. Nevertheless, it pays to inspect the angular distribution of all regenerated events for each T interval (Fig. 9), which shows rather clearly the effect of the interference, independently from the K_L normalization. With the K_L decay normalization, we can plot $\Delta N_{TR}(T)/\Delta N^0(T)$ (see Figs. 10 and 12).

As reported in a separate paper,²² a scattering experiment on charged kaons gave the results of Table IX for the regeneration amplitude in iron from K_L of 0.785 BeV/c. Making use of this information (actually of the more detailed information giving χ^2 versus values of $|f_{21}|$ and $\text{arc } f_{21}$), we obtain the χ^2 -versus- δ curve of Fig. 11. The value of δ is, from this experiment, measured to be 0.42 ± 0.04 in agreement with the more accurate values of Refs. 13 and 15 of Table I. (The error quoted here does not include the errors on $|f_{21}|$ and φ_{21} ; see Table IX.) We have assumed that $|f_{21}|$ is proportional to p within the momentum interval of 600 to 900 MeV/c, and that the regeneration phase φ_{21} is constant in this momentum range.

There seems to be no question about the sign of δ as far as statistical errors are concerned. Only the presence of a large unknown systematic error could reverse the sign. That this is not the case, however, can be seen from the following consideration.

²² W. A. W. Mehlhop, R. H. Good, O. Piccioni, R. A. Swanson, S. S. Murty, T. H. Burnett, C. H. Holland, and P. Bowles (to be published).

TABLE IX. $p = 785$ MeV/c, K^+ and K^- scattering on iron nucleus.^a

$V^+ = 14.4 \pm 2.1$	$V^- = -31.7 \pm 2.9$
$W^+ = -23.2 \pm 1.9$	$W^- = -33.0 \pm 5.8$
$f(K^0, 0^0) = f^+(0) = -9.34 + i22.71$	$f(\bar{K}^0, 0^0) = f^-(0) = 13.78 + i33.23$
$ f_{21} = 12.7 \pm 1.0$	
$\varphi_{21} = -155.5^\circ \pm 6.0^\circ$	
$\text{Re } f_{21} = -11.56$	
$\text{Im } f_{21} = -5.26$	
$ f_{22} = 28.06 \pm 3.0$	
$\varphi_{22} = 85.5^\circ \pm 3.5^\circ$	
$\text{Re } f_{22} = 2.22$	
$\text{Im } f_{22} = 27.97$	
$\sigma_{21} = 44.57 \pm 5.0$ mb	
$\sigma_{11} = \sigma_{22} = 272.64 \pm 28.0$ mb	
$(\sigma^1)_{\text{tot}} = (\sigma^2)_{\text{tot}} = 894.44 \pm 91.0$ mb	

^a Potentials are in units of MeV; scattering amplitudes in fermis.

If we assume a value for δ , the experiment can furnish the magnitude and phase of f_{21} . Taking $\delta = 0.46 \pm 0.03$ (combined value of Refs. 13 and 15), we get $|f_{21}| = 11.25 \pm 0.90$ F ($p = 780$ MeV/c) and $\varphi_{21} = -150.0^\circ \pm 11.5^\circ$. (See Figs. 12 and 13.)

This agrees very well with the values of Table IX obtained from the scattering experiment. A systematic cause which would invalidate our results about the sign of δ would of necessity produce a large error in the determination of the phase of f_{21} in either one of the two experiments, and it is quite inconceivable that the phase value would then fall in the narrow range appropriate

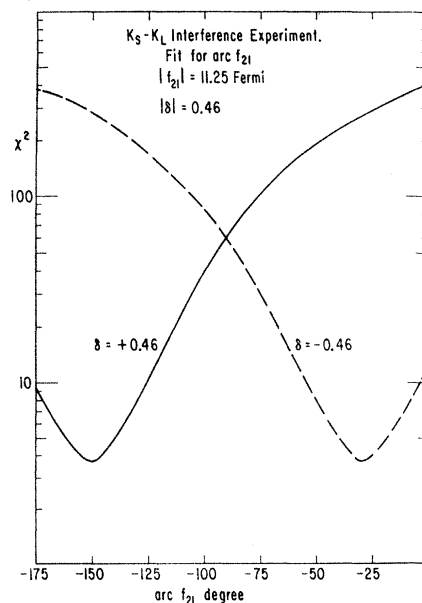


FIG. 13. Using an input value of $|f_{21}| = 11.25$ F, a mass difference of $\delta = +0.46$ (K_L heavier than K_S), the regeneration experiment gives $\varphi_{21} = -150^\circ \pm 11.5^\circ$. If we use $\delta = -0.46$ (K_L lighter than K_S), the regeneration experiment gives $\varphi_{21} = -30^\circ \pm 11^\circ$, which will be in contradiction to the value of phase obtained from the scattering experiment, viz., $\varphi_{21} = -155.5^\circ \pm 6.0^\circ$ (see Table IX).

for the opposite sign, with the appropriate value for the amplitude f_{21} . We thus believe that the question of the sign of δ is definitely answered.

Interference in Diffraction Scattering

It is interesting to note that an interference (this time constructive) due to the superposition of three amplitudes is visible in the scattered K_S^0 decays. Following the same line of reasoning as that of Ref. 3, we observe that at a depth x inside the regenerator (that is, at a distance $D+x$ from the source), we can distinguish [as we have done for the distance $(D+L)$] three amplitudes of undeflected waves: the original K_S , which we can indicate as $o(D+x)|K_S\rangle$, the transmission-regenerated K_S , $t(D+x)|K_S\rangle$, and the original K_L , $l(D+x)|K_L\rangle$. Here o , t , and l are the functions representing the propagation of the respective amplitudes.

After the scattering at x , in general at an angle θ different from zero, the scattered wave is

$$f_{11}(\theta)o(D+x)|K_S\rangle + f_{21}(\theta)l(D+x)|K_S\rangle + f_{11}(\theta)[t(D+x)|K_S\rangle + l(D+x)|K_L\rangle],$$

where $f_{11}(\theta)$ is the elastic scattering amplitude $f_{11}(\theta) = \frac{1}{2}[f^+(\theta) + f^-(\theta)]$, $f^+(\theta)$ and $f^-(\theta)$ being the amplitudes for positive and negative strangeness, respectively. The last two terms represent the transmission-regenerated amplitude in equilibrium with K_L up to the depth x , and the K_L amplitude, respectively.

In crossing the remaining $(L-x)$ thickness of the plate,

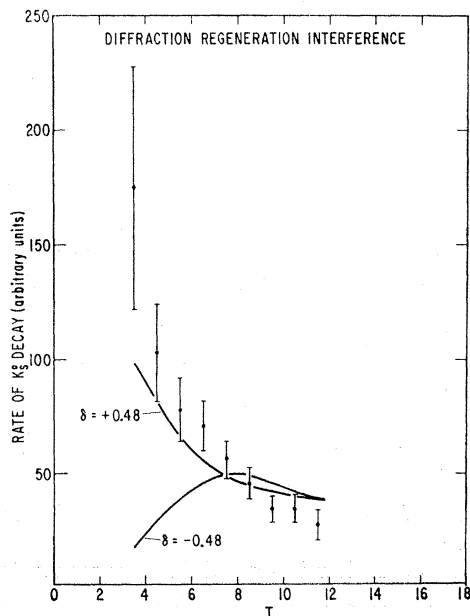


FIG. 14. Interference in diffraction scattering for 6-cm data and 3-cm data combined. The rate of K_S^0 decays is plotted against T . The curves shown are the best fit for $\delta > 0$, $\delta < 0$, respectively. Diffraction scattering are defined as events having $\cos(\theta p/760.0)$ between 0.998 to 0.990.

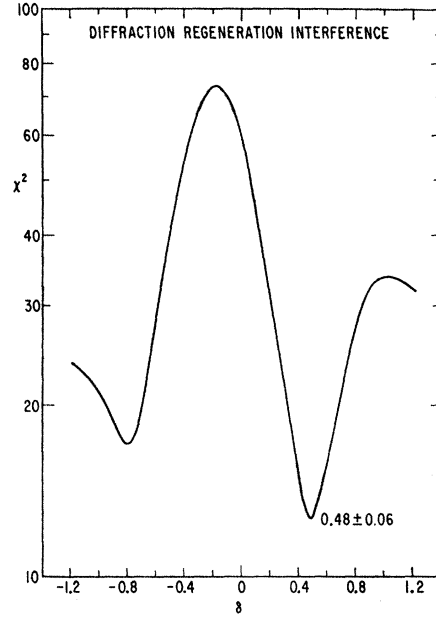


FIG. 15. Plot of χ^2 versus δ for the interference in diffraction scattering.

transmission regeneration from the K_L amplitude continues, so that the *sum* of the last two terms gives rise to the amplitude

$$f_{11}[t(D+L)|K_S\rangle + l(D+L)|K_L\rangle],$$

where the first term is equal to the scattering amplitude f_{11} times the same transmission-regenerated amplitude ψ_{LS} of Eq. (2).

Thus, the amplitude of $|K_S\rangle$, at the exit of the regenerator, is the sum of three amplitudes:

$$f_{11}(\theta)\exp[ik_s(D+L) - L/2\mu - (D+L)/2\Lambda] + f_{11}(\theta)A(L) \times \exp[ik_s(D+L) - L/2\mu - i\delta D/\Lambda] + f_{21}(\theta) \times \exp[ik_s(D+L) - L/2\mu - i\delta(D+x)/\Lambda - (L-x)/2\Lambda].$$

One recognizes that the sum of the first two amplitudes is exactly f_{11} times the amplitude which we study in the transmission interference effect, and which approaches zero at $T=5.5$ (Fig. 10).

Figure 14 shows the observed intensity of 2π decays versus T for 6-cm and 3-cm data combined.

The theoretical fit (Fig. 15) obviously favors a positive value of δ (K_L^0 heavier than K_S^0) and is in agreement with the transmission data.

We also want to remark that because f_{11} is, to a good approximation, a purely imaginary number, the difference $\arg f_{11} - \arg f_{21}$ is about $\frac{1}{2}\pi - \arg f_{21}$, while $\arg l - \arg t f_{21} = -\frac{1}{2}\pi - \arg f_{21}$. It is then easy to see that, for a thin regenerator, the interference in the diffraction regeneration produces a maximum at a value of D for which the transmission regeneration goes through a minimum.

CONCLUSIONS

It is quite comfortable to recall that other experiments²³⁻²⁵ have furnished evidence for a mass difference of the same sign as that demonstrated in this paper. We refer the reader to the original works for the description of the ingenious methods used in those experiments.

The proof of the interference effect shows that the 2π states from the regenerated K_{LS} are quantum-mechanically identical to the original K_S decays. On the other hand, since other evidence, also by interference, shows quantum identity between the regenerated K_{LS} and K_L in 2π decay, it follows that also K_L and K_S should interfere in their 2π mode. As a consequence, K^0 and \bar{K}^0 decay in 2π in a slightly but definitely different way—the K^0 having a minimum at $T \sim 11$, while the \bar{K}^0 has a minimum at $T \approx 13$.

Preliminary direct confirmation of this “direct” CP violation has been reported by Bohm *et al.*²⁶

Beside having an interest of its own, the sign of δ plays an important role in the CP -violating phenomena of K^0 's. One can trace the reason for this to the fact that the quantity $\epsilon = (p-q)/2p$ (Wu and Yang²⁷), when the contribution of CP violation in three-body decays is neglected, originates in the same fashion as a transmission-regenerated amplitude in a thin, long medium composed of nuclei with purely imaginary f_{21} [see Eq. (3) for $L \rightarrow \infty, \mu \rightarrow \infty$], namely,

$$\epsilon = M_i / (-i\delta + \frac{1}{2}i).$$

The sign of δ is thus important in determining the phase of ϵ .

A recent analysis by Bennett, Nygren, Saal, and Steinberger²⁸ of the latest experimental information on the amplitudes of $K_L \rightarrow \pi^\pm + e^\mp + \nu$ (Dorfan *et al.*,²⁹ Bennett *et al.*³⁰) has also furnished the phase of ϵ . The authors find disagreement with the existing data on the phase shift ($\delta_2 - \delta_0$) of the two-pion system if they take $\delta > 0$. This situation presents a puzzle.

²³ G. W. Meisner, B. B. Crawford, and F. S. Crawford, Jr., *Phys. Rev. Letters* **17**, 492 (1966).

²⁴ J. Canter, Y. Cho, A. Engler, H. E. Fisk, R. W. Kraemer, C. M. Melzer, D. G. Hill, D. K. Robinson, and M. Sakitt, in *Proceedings of the Thirteenth International Conference on High-Energy Physics, Berkeley, 1966* (University of California Press, Berkeley, 1967); sign of the K_L - K_S mass difference.

²⁵ J. V. Jovanovich, T. Fujii, F. Turkot, and M. Deutsch, *Phys. Rev. Letters* **17**, 1075 (1966).

²⁶ A. Bohm, C. Rubbia, J. Steinberger, and H. Ticho, in *Proceedings of the Heidelberg International Conference on Elementary Particles, Heidelberg, 1967*, edited by H. Filthuth (John Wiley & Sons, Inc., New York, 1968).

²⁷ Tai Tsun Wu and C. N. Yang, *Phys. Rev. Letters* **13**, 380 (1964).

²⁸ S. Bennett, D. Nygren, H. Saal, J. Steinberger, and J. Sunderland, *Phys. Rev. Letters* **19**, 997 (1967).

²⁹ D. Dorfan, J. Enstrom, D. Raymond, M. Schwartz, S. W. Jicki, D. H. Miller, and M. Paciotti, *Phys. Rev. Letters* **19**, 987 (1967).

³⁰ S. Bennett, D. Nygren, H. Saal, J. Steinberger, and J. Sunderland, *Phys. Rev. Letters* **19**, 993 (1967).

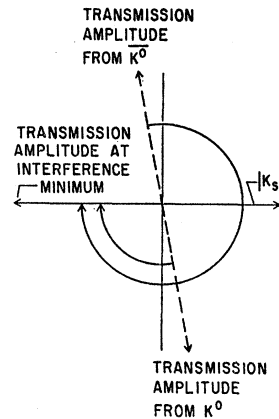


FIG. 16. Phase relations between the amplitudes of $|K_S\rangle$ and of $|K_{LS}\rangle$ for a beam of K^0 and \bar{K}^0 , respectively.

However, it appears to us that more accurate data on most of the other relevant quantities are indeed needed, because the conclusion that $\delta = M_L - M_S > 0$ seems to us inevitable.

We finally want to emphasize that the demonstration of the interference between $|K_{LS}\rangle$ and $|K_S\rangle$ opens the door for studies of higher accuracy, such as the regeneration from atomic electrons. This type of regeneration was initially estimated by Zeldovich,³¹ following a suggestion by Feinberg³² that neutral K mesons might have an electrical form factor, leading to a finite K^0 -electron scattering cross section. Zeldovich assumed that the value of the charge average square radius $\langle r^2 \rangle$ defined by $\langle r^2 \rangle = (1/e) \int r^2 dq$, where dq is the net charge at a radius r , is about $(\hbar/m_\pi c)^2$, and he hoped that the regeneration by electrons would experimentally be observed by an accurate determination of the intensity of the regeneration itself.

Our interference method allows now a much more sensitive detection of that phenomenon, by measuring the phase of the regeneration, which should be shifted by the electron-regeneration amplitude.

The shift could be evidenced by an accurate comparison of the regeneration phase with the phase obtained from K^+ , K^- scattering and with the phase obtained from the interference effect in the diffraction regeneration.

For our present work, the effect expected is about 1° , which is far too small considering our error. An effect 30 times less than that would be expected on the basis of the theory of dominance of vector mesons in electromagnetic interactions of hadrons which predicts for $\langle r^2 \rangle$ a value of $7 \times 10^{-28} \text{ cm}^2$ according to Kroll, Lee, and Zumino.³³

On the other hand, several improvements to the experiments can be made which can help to reduce the

³¹ Y. B. Zeldovich, *Zh. Eksperim. i Teor. Fiz.* **36**, 1381 (1959) [English transl.: *Soviet Phys.—JETP* **36**, 984 (1959)].

³² G. Feinberg, *Phys. Rev.* **109**, 1381 (1958).

³³ Norman M. Kroll, T. D. Lee, and Bruno Zumino, *Phys. Rev.* **157**, 1376 (1967).

error in the measurement of the phase. We cannot go into all details in this paper.

Finally, we want to remark that an experiment of better accuracy than this could compare the interference minimum for K^0 's (from K^+ charge exchange) with the minimum of \bar{K}^0 's (from K^- charge exchange). The two minima (Fig. 16) should be π/δ apart, *independently of the phase of the regeneration amplitude*, thus allowing an accurate determination of the mass difference δ . Relatively intense K^- beams are, of course, needed for this type of measurement.

ACKNOWLEDGMENTS

We thank Dr. Edwin M. McMillan for the courteous hospitality and the fine collaboration we enjoyed while working at the Lawrence Radiation Laboratory. Laurence Littenberg was very cooperative in assisting us during the run. Our gratitude also goes to our head scanner Nancy Drown and our scanners J. Carrasco, J. Chapman, S. Grissom, C. Lee, J. Ludwig, and G. Whitley, and to our secretary Mary Terrell. The fine work of Noel Bartlett in building the cameras is also appreciated.

Vector Fields and Current Commutators. II

DAVID G. BOULWARE*

Physics Department, University of Washington, Seattle, Washington 98105

(Received 16 February 1968)

In a previous paper with the same title, it was shown that divergence conditions are equivalent to current commutation relations. Some of the assumptions which were made are shown to follow from more fundamental postulates.

THERE have been several papers^{1,2} showing that divergence conditions involving vector fields imply that the partially conserved currents obey current algebra commutation relations.³ These have generally made some assumptions concerning the vanishing of specific commutators or a limitation on the number of derivatives of δ functions which can occur. In this paper, it is shown that all the usual commutators⁴ follow from the assumption that the vector field obeys canonical (c number) commutation relations and the divergence conditions of the currents to which they are coupled. The notation of the preceding paper by Brown and the author² will be used throughout. In that paper the basic equations,⁵

$$G_a^{\mu\nu} = \partial^\mu B_a^\nu - \partial^\nu B_a^\mu, \quad (1)$$

$$\partial_\nu G_a^{\mu\nu} + m^2 B_a^\mu = g j_a^\mu, \quad (2)$$

$$\partial_\mu j_a^\mu = d_a + ig C_{abc} B_{b\mu} j_c^\mu, \quad (3)$$

and the canonical commutators,

$$[G_a^{0k}(0, \mathbf{r}), B_b^l(0, \mathbf{r}')] = i\delta^{kl}\delta_{ab}\delta(\mathbf{r} - \mathbf{r}'), \quad (4)$$

$$[B_a^k(0, \mathbf{r}), B_b^l(0, \mathbf{r}')] = 0 = [G_a^{0k}(0, \mathbf{r}), G_b^{0l}(0, \mathbf{r}')], \quad (5)$$

are used to prove the current-algebra commutation relations

$$[j_a^0(0, \mathbf{r}), j_b^0(0, \mathbf{r}')] = C_{abc} j_c^0(\mathbf{r})\delta(\mathbf{r} - \mathbf{r}') \quad (6)$$

and

$$[j_a^0(0, \mathbf{r}), j_b^l(0, \mathbf{r}')] = C_{abc} j_c^l(\mathbf{r})\delta(\mathbf{r} - \mathbf{r}') - i\rho_{ab}{}^{kl}(\mathbf{r}')\partial_k\delta(\mathbf{r} - \mathbf{r}'), \quad (7)$$

subject to the assumptions that

$$[B^k(0, \mathbf{r}'), j_b^\mu(0, \mathbf{r}')] = 0 \quad (8)$$

and

$$[d_a(0, \mathbf{r}), G_b^{0k}(0)] = 0 = [d_a(0, \mathbf{r}), B_b^k(0, \mathbf{r}')]. \quad (9)$$

The purpose of this paper is to prove that assumption (8) may always be taken to be true by a trivial redefinition of j ; assumption (9) cannot be dropped since otherwise, for example, d_a could be taken to be $-igC_{abc}B_b j_c$, and the current commutators would vanish except for the Schwinger term.

The method used is simply to require that the commutators be consistent with the Lorentz transformation properties of the fields involved. The relevant commutators with P^0 and J^{0k} , the generators of time transla-

* Supported in part by the U. S. Atomic Energy Commission under Grant No. A.T.(45-1)1388B.

¹ M. Veltman, Phys. Rev. Letters **17**, 554 (1966); M. Nauenberg, Phys. Rev. **154**, 1455 (1967); J. S. Bell, Nuovo Cimento **50A**, 129 (1967); S. G. Brown, Phys. Rev. **158**, 1444 (1967).

² D. G. Boulware and L. S. Brown [Phys. Rev. **156**, 1724 (1967)] which will subsequently be referred to as (I).

³ M. Gell-Mann, Physics **7**, 63 (1964).

⁴ The status of the commutator of the space components of the vector field with the time component of the current is still open to question; this point is discussed later.

⁵ The metric $(-1, 1, 1, 1)$ is used; C_{abc} are the totally antisymmetric structure constants of the internal symmetry group.